STRUCTURAL CHEMISTRY

Volume 77 (2021)

Supporting information for article:

Transition-metal complexes of group 12 with 1,1′-bis(phosphanyl)ferrocene ligands

Karan Chaudhary, Manoj Trivedi, Dhanraj T. Masram and Nigam P. Rath

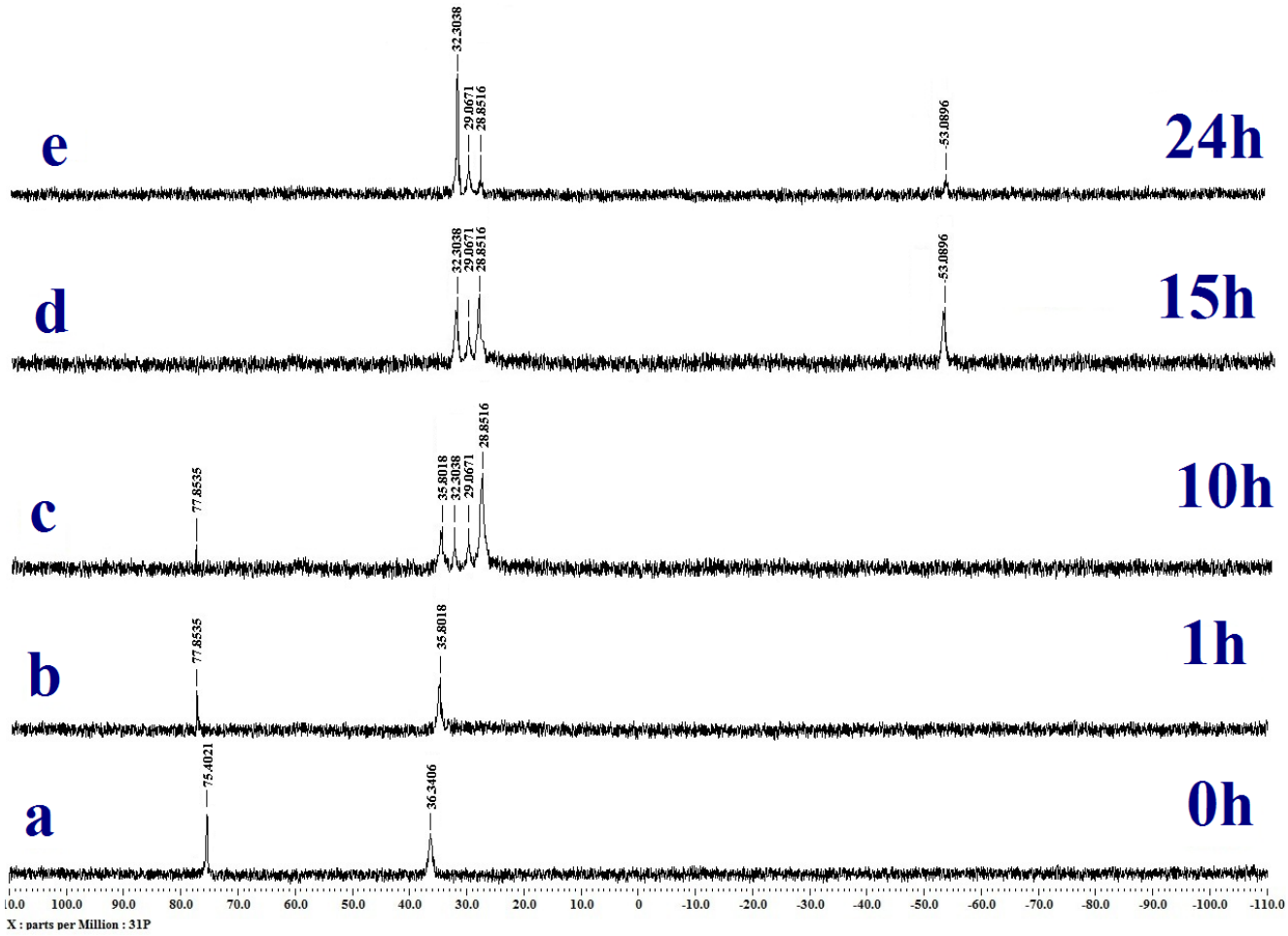

Figure S1 Time-resolved ^{31}P NMR spectra recorded directly from the reaction mixture in $CDCl_3$ by using phosphoric acid as an external standard; 0h (a), 1h (b), 10h (c), 15h (d), and 24h (e) of PdI_2 (0.011 g; 3.1 x 10^{-2} mmol) containing dppdtbpf (1.028 g, 2.0 mmol) was treated with aqueous KOH (25 wt %, 18 mL) and 1,2-dibromoethane (0.999 g, 5.32 mmol) containing KI (0.045 g, 0.27 mmol). The signals at 75.40, 36.34 corresponds to dppdtbpf; 77.85, 35.80 corresponds to Pd(κ^1-dppdtbpf)I_2; 32.30, 29.06 corresponds to dppOdtbpf and 28.85, -53.08 may be due to $(dppdtbpfH_2)^{2+}$.

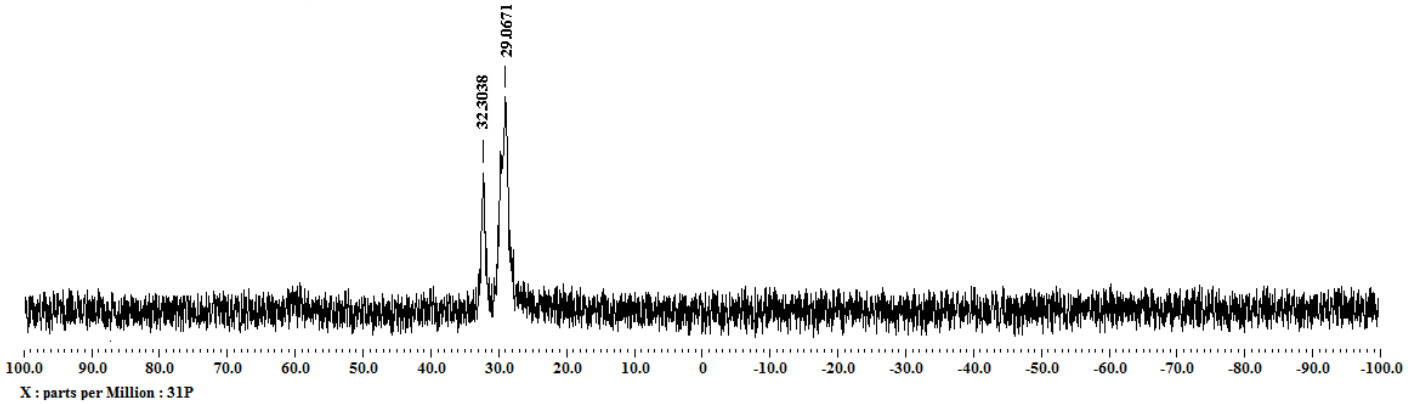

Figure S2 ^{31}P NMR spectrum of **L^{1}** in $CDCl_3$.

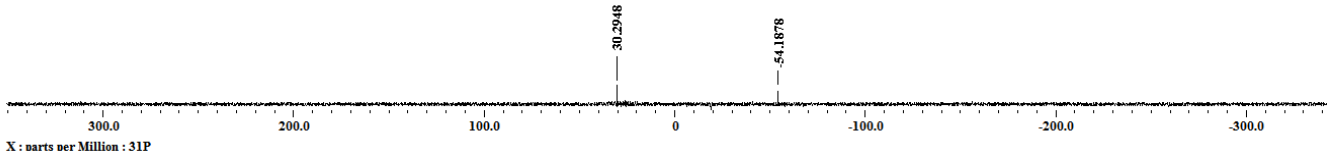

Figure S3 ^{31}P NMR spectrum of **1** in $CDCl_3$.

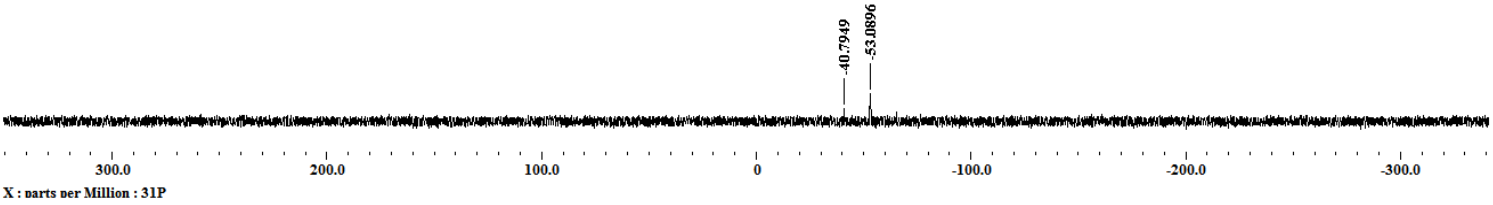

Figure S4 ^{31}P NMR spectrum of **2** in $CDCl_3$.

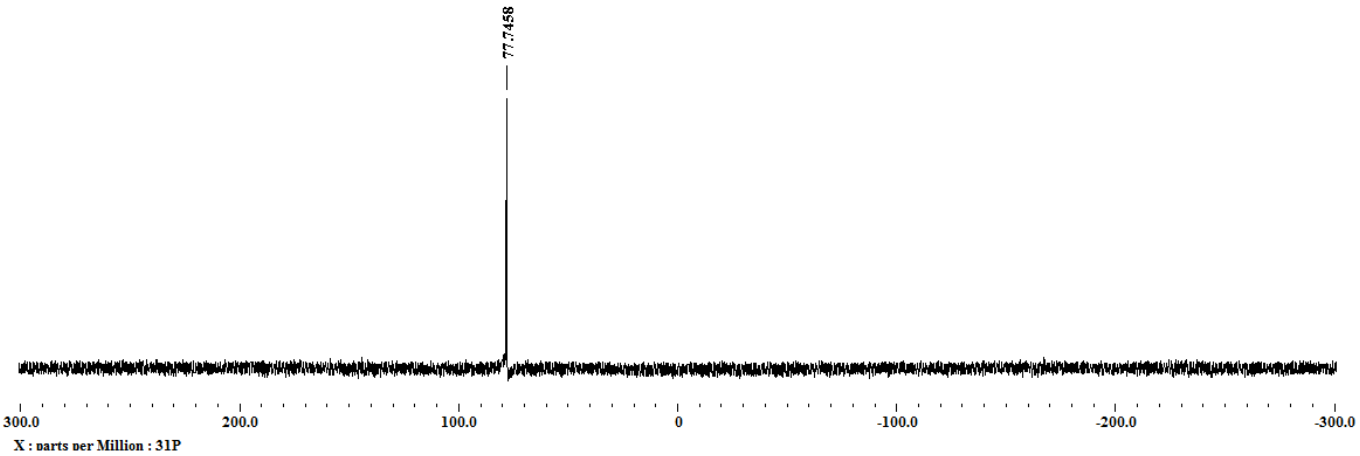

Figure S5 ^{31}P NMR spectrum of **3** in $CDCl_3$.

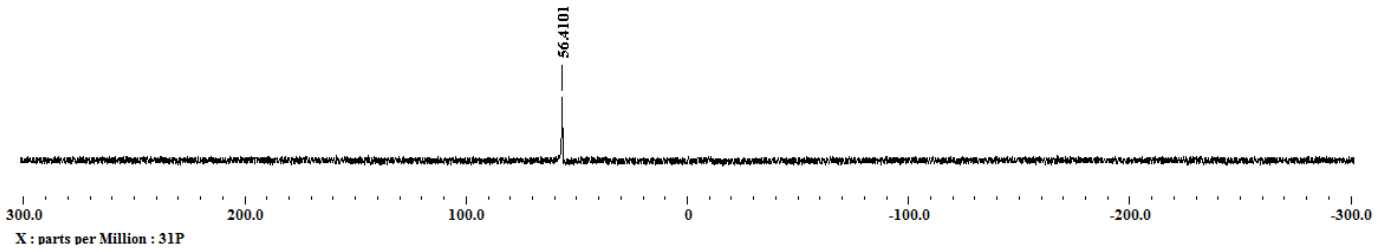

Figure S6 ^{31}P NMR spectrum of **4** in $CDCl_3$.

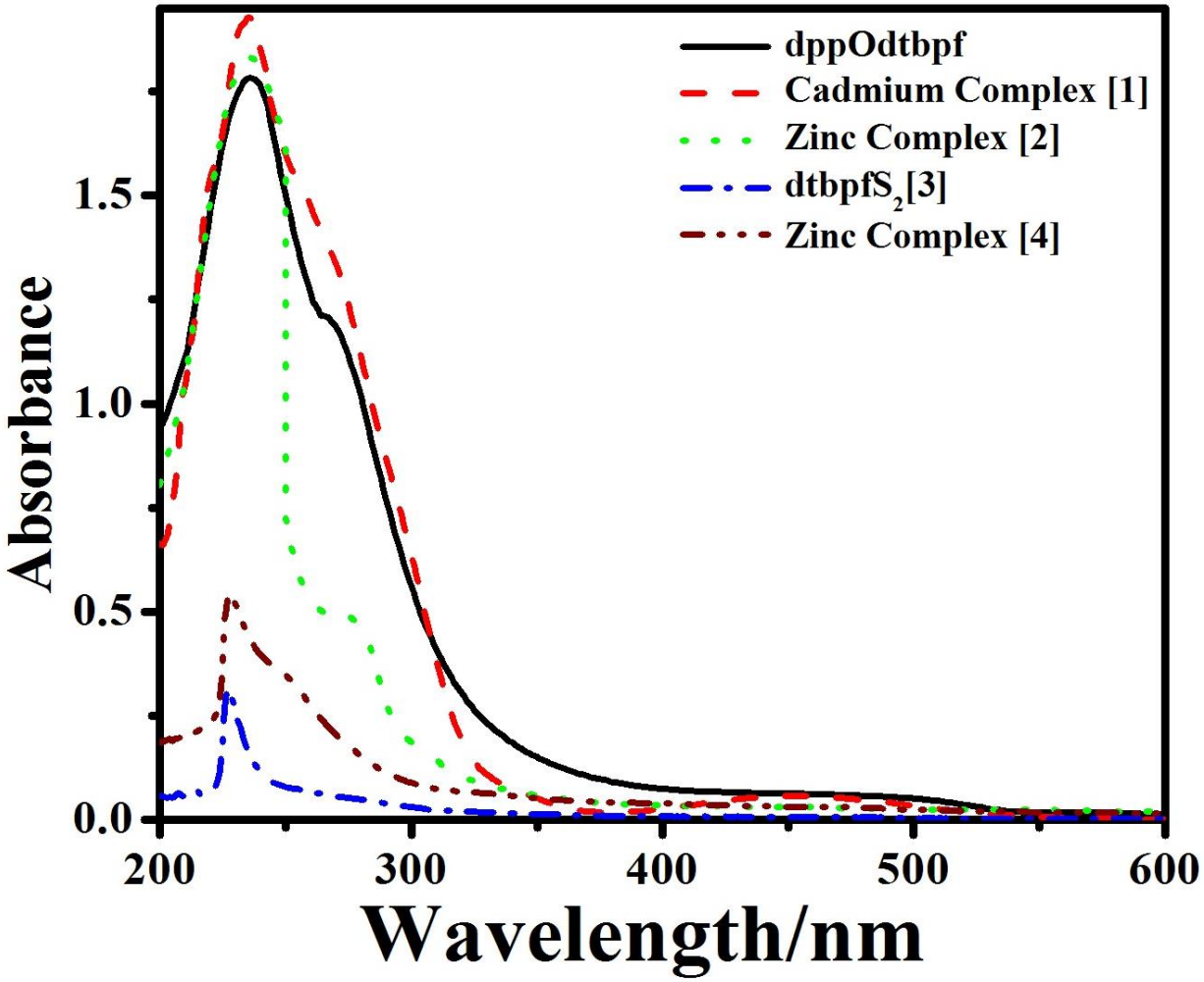

Figure S7 UV-Vis spectra of all compounds in CH_2Cl_2.

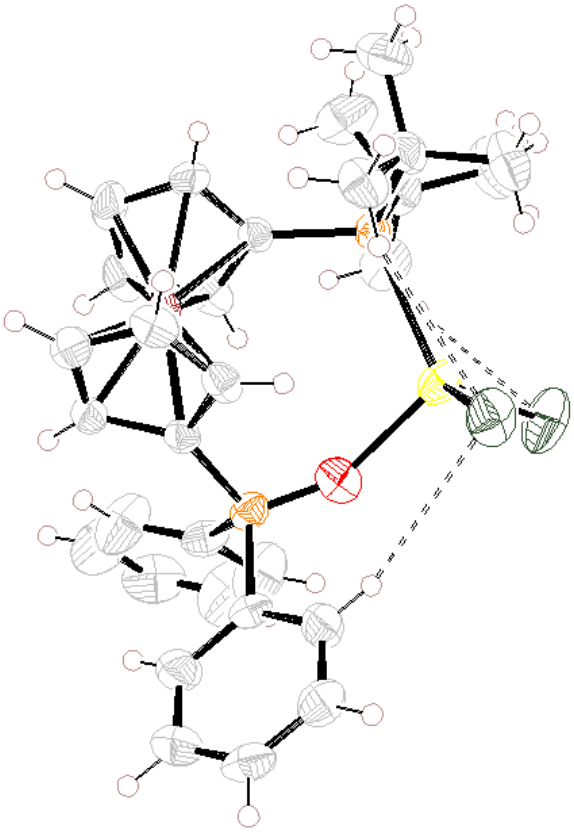

Figure S8 Ortep diagram of **1** showing C-H···Cl hydrogen bond interactions.

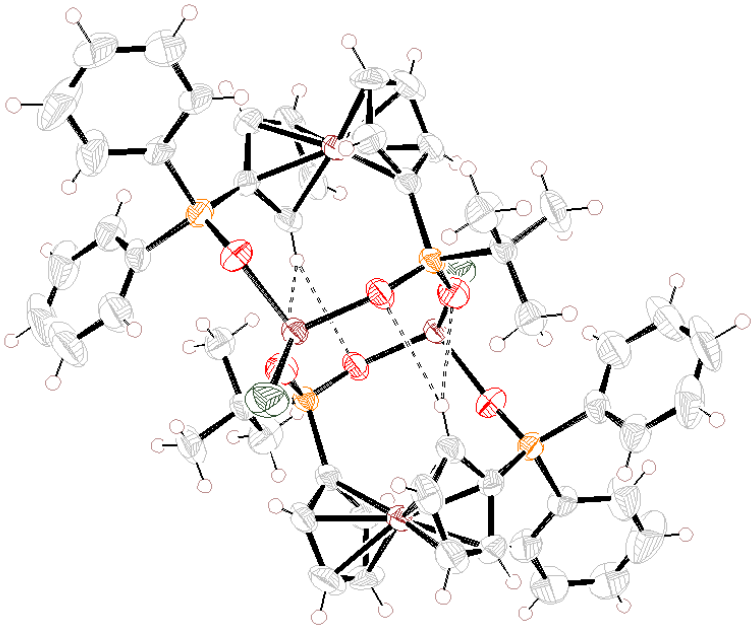

Figure S9 Ortep diagram of **2** showing C-H···O hydrogen bond interactions.

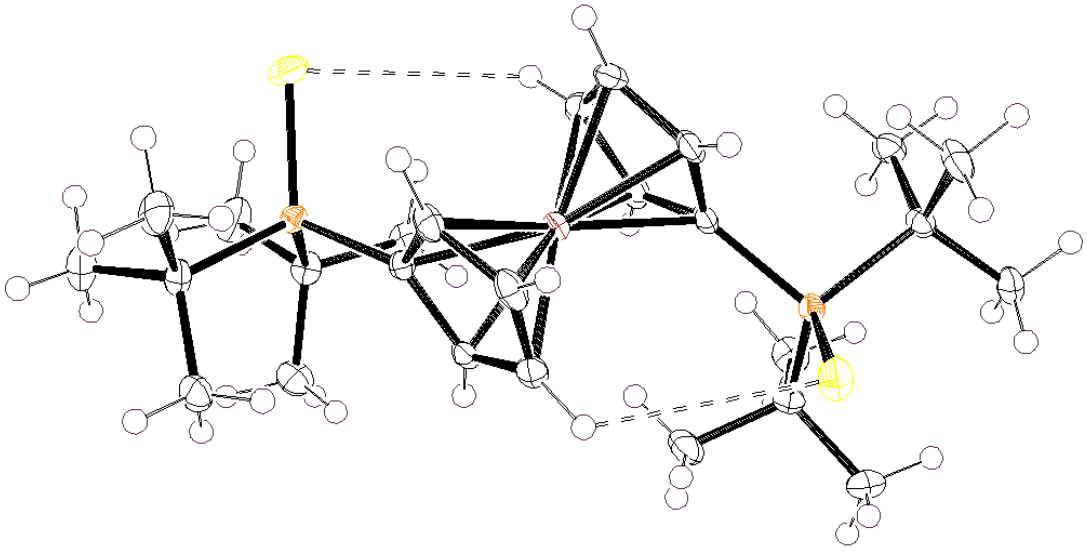

Figure S10 Ortep diagram of **3** showing C-H···S hydrogen bond interactions.

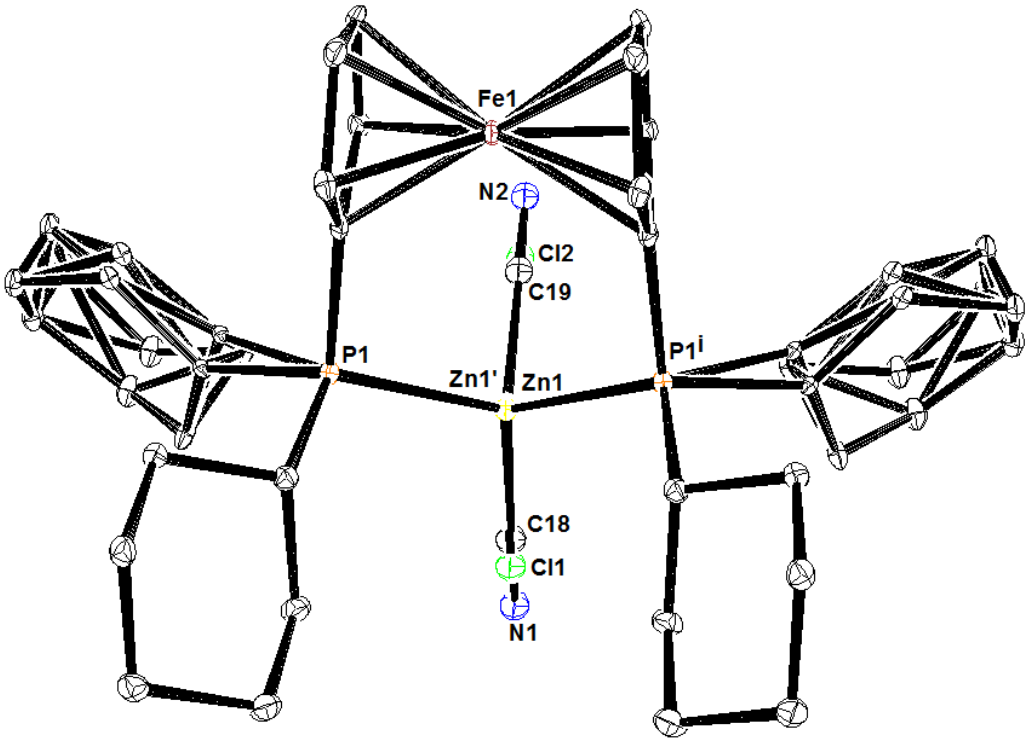

Figure S11 Thermal ellipsoid plot of compound **4** (30% probability). H atoms are omitted for clarity.

S1. Electrochemistry

The electrochemical properties of new compounds were investigated by cyclic voltammetry in CH_2Cl_2 at room temperature (RT) and the redox data are presented in Table S1. The cyclic voltammogram of dppOdtbpf was analyzed and the potential at which oxidation occurs (E^0) is 0.12 V relative to $Fc^{+/0}$. This is similar to the potentials at which oxidation of the closely related dppdtbpf derivatives take place (0.11 V vs. $Fc^{+/0}$) (Kahn *et al.*, 2009). The oxidative electrochemistry of cadmium compound **1** was also investigated. The oxidation of **1** is chemically and electrochemically quasi-reversible. The potential at which oxidation occurs is +0.54 V (Figure S12). The electrochemical oxidation of compound **2** is quasi-reversible and occurred at potentials 0.37 V and 1.27 V, respectively (Figure S13). The reversibility of these waves suggests that the oxidation of the iron centre has minimal impact on the O-Zn bonds (Hartlaub *et al.*, 2017). The electrochemistry of compound **3** has been previously described by Nataro *et al.* (Blanco *et al.*, 2006). We have found similar findings, and it shows the one chemically and electrochemically reversible wave (Figure S14). Compound **4** is also quasi-reversible and occurred at potentials 0.81 V and -0.55 V, respectively (Figure S15).

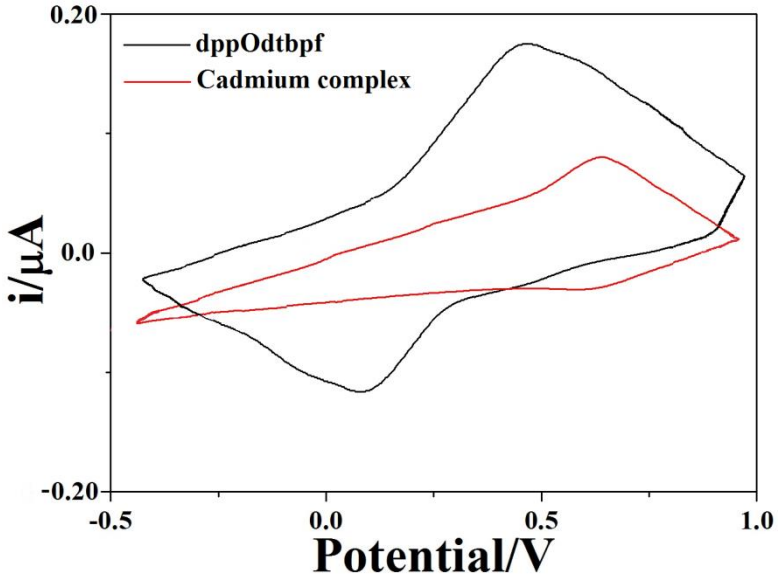

Figure S12. Cyclic voltammograms for dppOdtbpf and cadmium compound **1** in CH_2Cl_2/0.1 M $[NBu_4]PF_6$ at 100 mVs^{-1} scan rate.

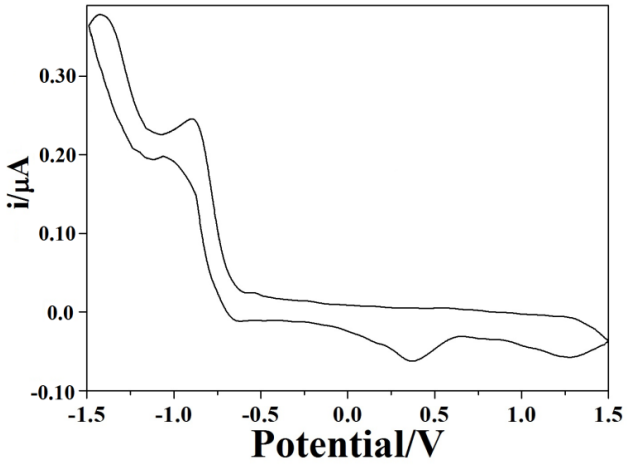

Figure S13. Cyclic voltammogram for $(ZnOCl(\kappa^2\text{-}O,O\text{-}Ph_2POFcPO_2(t\text{-}Bu))_2$ in CH_2Cl_2/0.1 M $[NBu_4]PF_6$ at 100 mVs^{-1} scan rate.

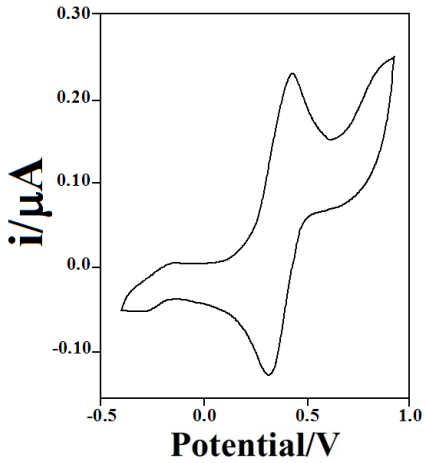

Figure S14. Cyclic voltammogram for $dtbpfS_2$ in CH_2Cl_2/0.1 M $[NBu_4]$ PF_6at 100 mVs^{-1} scan rate.

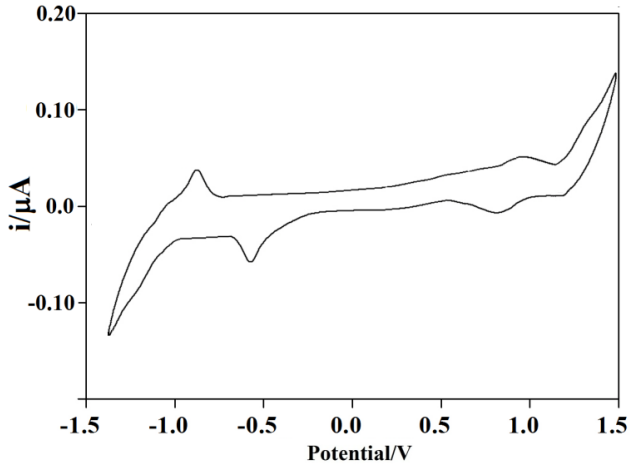

Figure S15. Cyclic voltammogram for $Zn(CN)_2(\kappa^2\text{-dcpf})$ in CH_2Cl_2/0.1 M $[NBu_4]PF_6$ at 100 mVs^{-1} scan rate.

Table S1 Electrochemical data in dichloromethane solution/0.1 M $[NBu_4]PF_6$ at 298 K.

Compound	Oxidation $^{a}E_{pa}$/V *vs.* SCE	Reduction $^{b}E_{pc}$/V *vs.* SCE
dppOdtbpf	+0.12	+0.48
$[CdCl_2(\kappa^2$-P,O-dppOdtbpf)] (**1**)	+0.54	+0.64
$[ZnOCl(\kappa^2$-O,O-$Ph_2POFcPO_2(t$-Bu))$]_2$ (**2**)	+0.37, 1.27	-0.89, -1.44
$dtbpfS_2$ (**3**)	+0.36	+0.46
$[Zn(CN)_2(\kappa^2$-dcpf)] (**4**)	+0.81,-0.55	-0.80, 1.12

$^{a}E_{pa}$ is the anodic peak potential of the reversible oxidation wave; $^{b}E_{pc}$ is the cathodic peak potential of the reversible oxidation wave.

References

Blanco, F. N., Hagopian, L. E., McNamara, W. R., Golen, J. A., Rheingold, A. L. & Nataro, C. (2006). *Organometallics*. **25**, 4292-4300.

Hartlaub, S. F., Lauricella, N. K., Ryczek, C. N., Furneaux, A. G., Melton, J. D., Piro, N. A., Kassel, W. S. & Nataro, C. (2017). *Eur. J. Inorg. Chem.***2017**, 424-432.

Kahn, S. L., Breheney, M. K., Martinak, S. L., Fosbenner, S. M., Seibert, A. R., Kassel, W. S., Dougherty, W. G. & Nataro, C. (2009). *Organometallics*. **28**, 2119-2126.

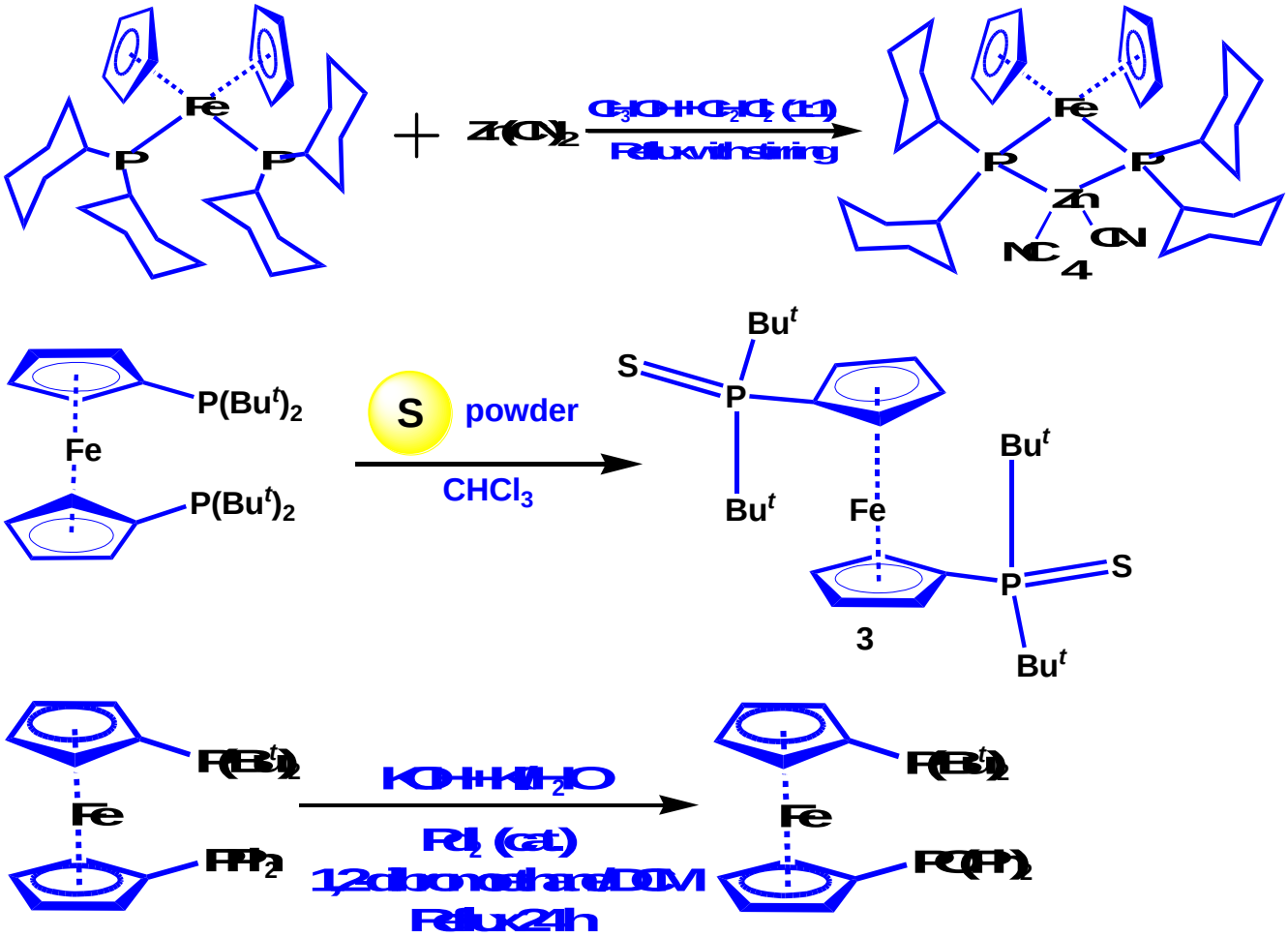
Fe
P
P
Zn
CN
NC
4
P(Bu^t)$_2$
Fe
P(Bu^t)$_2$
S
powder
CHCl$_3$
Bu^t
S
P
Bu^t
Fe
Bu^t
P
S
Bu^t
3